Journal of Thermal Analysis and Calorimetry, Vol. 85 (2006) 2, 417–424

A COMPARATIVE STUDY ON THE THERMAL DECOMPOSITION OF SOME TRANSITION METAL CARBOXYLATES

B. S. Randhawa and K. Gandotra*

Department of Chemistry, Guru Nanak Dev University, Amritsar, India

Thermal decomposition of transition metal malonates, $MCH_2C_2O_4{\cdot}xH_2O$ and transition metal succinates, $M(CH_2)_2C_2O_4{\cdot}xH_2O$ (*M*=Mn, Fe, Co, Ni, Cu, Zn) has been studied employing TG, DTG, DTA, XRD, SEM, IR and Mössbauer spectroscopic techniques. After dehydration, the anhydrous metal malonates and succinates decompose directly to their respective metal oxides in the temperature ranges 310–400 and 400–525°C, respectively. The oxides obtained have been found to be nanosized. The thermal stability of succinates have been found to be higher than that of the respective malonates.

Keywords: *metal malonates, metal succinates, SEM, thermal decomposition, thermogravimetry, XRD*

Introduction

The last three decades have witnessed a phenomenal progress in the field of thermal analysis especially in instrumentation and widening scope of its applications. The application of thermal techniques encompasses a wide spectrum of fields ranging from pure and applied sciences to technology. In fact, the data derived using thermoanalytical techniques have contributed significantly to the evolution of a large variety of high-tech materials used in the specialized areas of science and technology. As a result, thermal analysis has become a very popular tool in both academic and industrial organizations for characterization, performance evaluation and determination of process parameters of various types of materials. Thermal decomposition of metal carboxylates has become a subject of recent interest in view of their diverse applications. The appreciable complexing ability and ease of decomposition and availability at a reasonable cost, make them potentially useful as water proofing materials, flattening and softening agents, hydrogenation catalysts, greases, lubricants, cosmetics, pesticides, etc. [1, 2]. The final thermolysis products (metal oxides) are extensively used as catalysts, ceramic colorants, photoconductors and gas sensors [3–5]. Although a detailed study on thermal analysis has been reported for transition metal oxalates [6], a similar interest on respective malonates/succinates is lacking. The present investigation on thermolysis of transition metal (*M*=Mn, Fe, Co, Ni, Cu, Zn) malonate/succinates has been, therefore, undertaken with a view to study the effect of increasing carbon chain length (malonates→succinates) on their thermal stabilities.

Experimental

Transition metal malonates, $MCH_2C_2O_4{\cdot}xH_2O$ (*M*= Mn, Fe, Co, Ni, Cu, Zn) were prepared by mixing stoichiometric quantities of aqueous solutions of respective transition metal carbonates and malonic acid. The resultant solution was heated overnight at 60°C. The reaction mixture was cooled and filtered by using suction pump. After washing with ethanol and air-drying, the compound was stored in a desiccator. On the other hand, transition metal succinates, $M(CH_2)_2C_2O_4{\cdot}xH_2O$ (*M*= Mn, Fe, Co, Ni, Cu, Zn) were prepared by mixing with constant stirring the stoichiometric quantities of aqueous solutions of succinic acid and respective transition metal sulphate. The precipitates formed after sometime were isolated, washed with ethanol, allowed to air-dry and stored in a vacuum desiccator. The percentage of manganese in manganese malonate/succinate was determined titrimetrically using Eriochrome Black-T as indicator [7]. The content of iron in iron malonate/succinate was determined spectrophotometrically using 1,10-phenanthroline method [7]. The contents of cobalt, nickel, copper and zinc in respective malonates/succinates were determined electrogravimetrically [7]. The identity of these compounds was established by elemental analysis (Table 1).

For non-isothermal studies, simultaneous thermal analysis (TG-DTG-DTA) curves were recorded on a Stanton Redcraft (STA-780) model at a heating rate of 10°C min^{-1}. These studies were performed in static air atmosphere at USIC, IIT, Roorkee. The infrared spectra of transition metal succinates in the range 4000–200 cm^{-1} were recorded on PYE-UNICAM SP3-300 IR spectrophotometer using KBr matrix. The

* Author for correspondence: balwinderrandhawa@yahoo.co.in

1388–6150/$20.00

Akadémiai Kiadó, Budapest, Hungary
Springer, Dordrecht, The Netherlands

Table 1 Microanalytical data for various transition metal malonates and succinates

Compound	C/%	H/%	*M*/%
$MnCH_2C_2O_4{\cdot}2H_2O$	obs. 17.42 calc. 18.65	3.07 3.11	28.10 28.50
$Mn(CH_2)_2C_2O_4{\cdot}1.5H_2O$	obs. 24.10 calc. 24.24	3.21 3.53	27.56 27.78
$FeCH_2C_2O_4{\cdot}H_2O$	obs. 19.80 calc. 20.45	2.01 2.27	30.70 31.81
$Fe(CH_2)_2C_2O_4{\cdot}2.5H_2O$	obs. 21.84 calc. 22.21	3.92 4.15	24.03 25.81
$CoCH_2C_2O_4{\cdot}H_2O$	obs. 19.90 calc. 20.12	2.15 2.23	32.66 32.92
$Co(CH_2)_2C_2O_4{\cdot}4H_2O$	obs. 19.24 calc. 19.44	4.51 4.86	23.42 23.86
$NiCH_2C_2O_4{\cdot}2H_2O$	obs. 18.20 calc. 18.30	2.93 3.05	29.06 29.84
$Ni(CH_2)_2C_2O_4{\cdot}4H_2O$	obs. 19.20 calc. 19.45	4.73 4.86	22.86 23.79
$CuCH_2C_2O_4{\cdot}2H_2O$	obs. 17.69 calc. 17.86	2.84 2.98	30.00 31.50
$Cu(CH_2)_2C_2O_4{\cdot}2H_2O$	obs. 22.06 calc. 22.27	3.63 3.71	29.15 29.46
$ZnCH_2C_2O_4{\cdot}2H_2O$	obs. 16.39 calc. 17.73	2.81 2.95	31.80 32.02
$Zn(CH_2)_2C_2O_4$	obs. 28.26 calc. 28.74	2.15 2.39	37.80 38.92

room temperature X-ray diffraction (XRD) powder data were recorded at Soils Department, P.A.U., Ludhiana using nickel filtered CuK_α radiation. The scanning electron microscopic (SEM) studies for determining the particle size were carried out using JEOL scanning electron microscope at RSIC, Panjab University, Chandigarh. For iron carboxylates, Mössbauer studies were performed at Laboratoire de Physique, Université du Maine, France using conventional transmission spectrometer with constant acceleration drive and isomer shift values have been reported with respect to pure iron absorber.

Results and discussion

IR spectrum of manganese malonate dihydrate shows a broad band centered at about 3400 cm^{-1} due to ν_{OH} of lattice water. A shoulder at 2950 cm^{-1} is assigned to ν_{C-H} of malonate ligand. A strong band at 1585 cm^{-1} is due to $\nu_{asym(C=O)}$ whereas a sharp band at 1405 cm^{-1} alongwith a shoulder at 1460 cm^{-1} is attributed to $\nu_{sym(C=O)}$ of malonate group. Bands in the range 1210–985 cm^{-1} correspond to (O–H) bending mode. A sharp band at 815 cm^{-1} is associated with *cis*(C–H) wagging and distinct bands in the range 290–585 cm^{-1} indicate the presence of Mn–O (carboxylate) bonding [8]. The IR spectra of other transition metal carboxylates are almost similar to that of manganese malonate dihydrate.

The compoundwise discussion on thermolysis of various transition metal carboxylates follows.

Manganese malonate dihydrate, $MnCH_2C_2O_4{\cdot}2H_2O$

Figure 1 shows the simultaneous thermal analysis curves (TG-DTG-DTA) of manganese malonate dihydrate at a heating rate of 10°C min^{-1}. The compound undergoes decomposition in two steps. The first step is the dehydration, which commences at 163°C and completes at 230°C as indicated by a mass loss of 19% due to the removal of two water molecules. DTA and DTG show corresponding peaks at 205°C (endothermic) and 200°C, respectively, suggesting that thermal changes are accompanied by mass loss. The high temperature of dehydration indicates that both the water molecules are coordinated ones. The anhydrous compound remains stable upto 290°C as shown by an arrest in TG and then undergoes a rapid oxidative decomposition process as shown by a strong exotherm at 315°C followed by a sharp DTG peak. This rapid decomposition step leads to a mass loss of 62.5% at 330°C indicating the formation of manganese oxide, MnO (calc. loss=63%). The presence of manganese oxide as a final thermolysis product has been confirmed by XRD powder data which agree to that reported for MnO [9]. IR spectrum of the residue obtained by heating the parent complex isothermally at 400°C for 3 h shows characteristic bands in the range 300–540 cm^{-1} due to Mn–O bonding [10]. Manganese

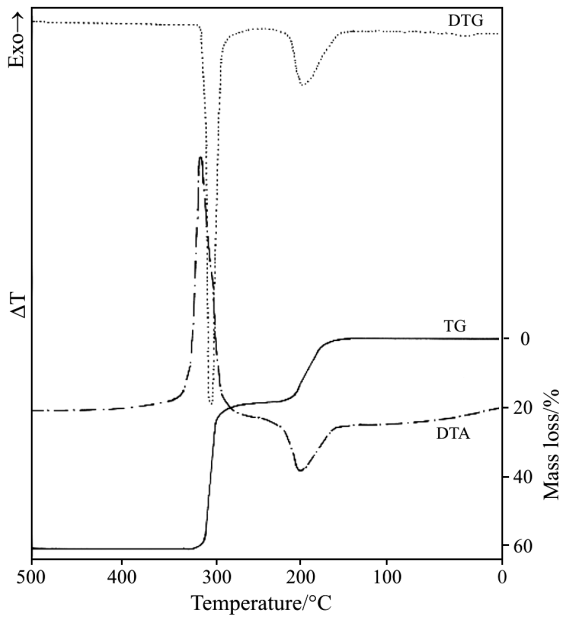

Fig. 1 Simultaneous TG-DTG-DTA curves of manganese malonate dihydrate

oxalate is also reported to decompose directly to manganese oxide without yielding carbonate as an intermediate [6]. SEM micrograph (Fig. 2) reveals the formation of MnO with an average particle size of 75 nm.

Manganese succinate sesquehydrate, $Mn(CH_2)_2C_2O_4 \cdot 1.5H_2O$

Figure 3 shows the simultaneous thermal analysis curves (TG-DTG-DTA) of manganese succinate sesquehydrate at a heating rate of 10°C min^{-1}. The compound undergoes decomposition in two steps. The first step is dehydration, which commences at 152 and completes at 215°C as indicated by a mass loss of 13% (calc. loss=13.6%). DTA and DTG show corresponding broad peaks centered at 205 (endothermic) and 208°C, respectively. The anhydrous compound remains stable upto 310°C and then undergoes an abrupt oxidative decomposition process as shown by a strong exotherm at 380°C via the formation of an unstable intermediate species (supported by a shoulder in DTA and DTG at 347°C). This decomposition step is associated with a mass loss of 64% at 420°C indicating the formation of manganese oxide, MnO (calc. loss=64%). The presence of manganese oxide as the final thermolysis product has been confirmed by XRD powder data which agree to that reported for MnO [9]. IR spectrum of the final residue resembles to that observed for respective malonate salt. MnO is reported to be stable upto 600°C [11].

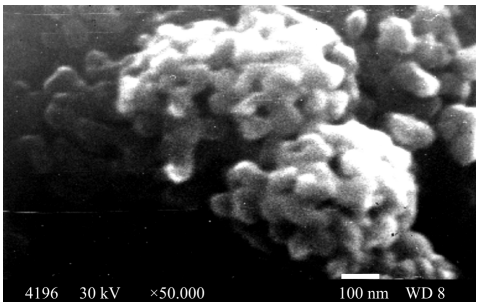

Fig. 2 SEM micrograph of the final thermolysis residue of manganese malonate dihydrate (MnO), sintered at 400°C for 3 h

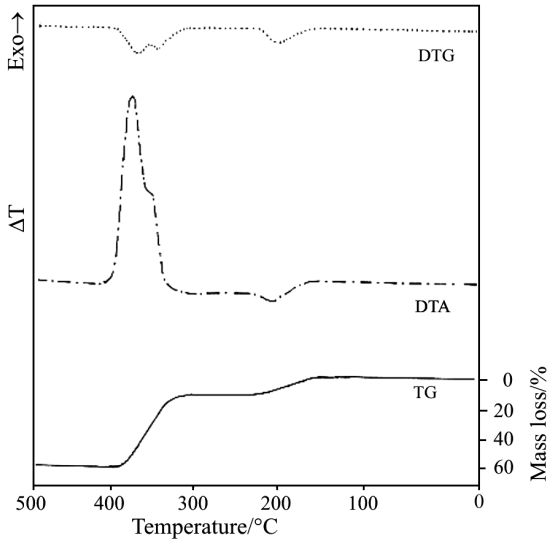

Fig. 3 Simultaneous TG-DTG-DTA curves of manganese succinate sesquehydrate

Ferrous malonate monohydrate, $FeCH_2C_2O_4 \cdot H_2O$

Figure 4 shows the simultaneous thermal analysis curves (TG-DTG-DTA) of iron(II) malonate monohydrate. The dehydration commences at 66 and completes at 204°C as shown by a mass loss of 10.0% due to the removal of one-water molecule (calc. loss= 10.2%). The anhydrous compound remains stable upto 269°C and starts decomposing gradually. After passing through multistep oxidative decomposition process (as supported by DTG peaks and an exothermic region from 269 to 484°C), it ultimately decomposed to oxide as shown by a mass loss 56% (calc. loss 56%). The identity of iron oxide has been confirmed by XRD powder pattern, which resembles to that reported for α-Fe_2O_3 [12]. IR spectrum of the residue obtained by calcining the parent complex isothermally at 500°C for 2 h shows small intense bands in the region 550–350 cm^{-1} due to ν(Fe–O). Mössbauer spectrum of the end product exhibits a six-line pattern (Fig. 5) with isomer shift and internal magnetic field values of 0.40 mm s^{-1} and 505 kOe, respectively. These parameters are in close agreement to those reported for α-Fe_2O_3 [13]. SEM micrograph (Fig. 6) reveals the formation of α-Fe_2O_3 with an average particle size of 88 nm. However, after sintering at 800°C for 3 h, the particle size increased to 600 nm (Fig. 7). An increase in particle size/diameter of α-Fe_2O_3 with increasing sintering temperature has also been reported in literature [14].

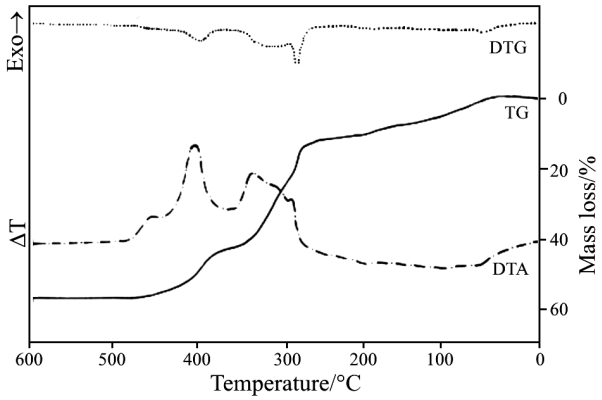

Fig. 4 Simultaneous TG-DTG-DTA curves of ferrous malonate monohydrate

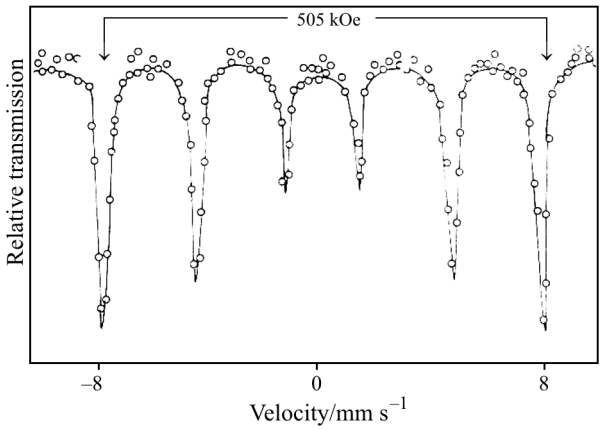

Fig. 5 Mössbauer spectrum of Fe(II) malonate monohydrate calcined at 500°C

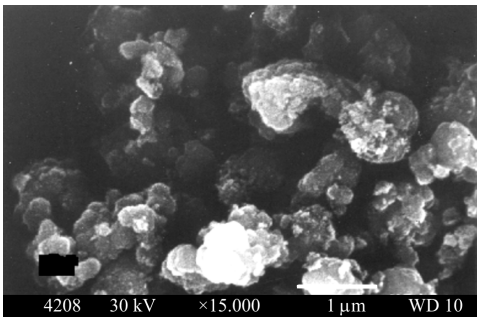

Fig. 6 SEM micrograph of the final thermolysis residue of Fe(II) malonate monohydrate (α-Fe_2O_3), sintered at 500°C for 3 h

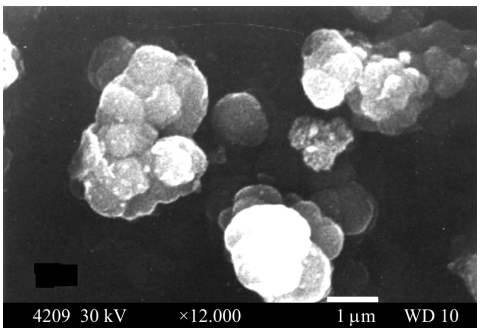

Fig. 7 SEM micrograph of the final thermolysis residue of Fe(II) malonate dihydrate (α-Fe_2O_3), sintered at 800°C for 3 h

Ferrous succinate sesterhydrate, $Fe(CH_2)_2C_2O_4 \cdot 2.5H_2O$

Figure 8 shows the simultaneous thermal analysis curves (TG-DTG-DTA) of ferrous succinate sesterhydrate at a heating rate of 10°C min^{-1}. The dehydration occurred in two steps. In the first step, there is a loss of 4% indicating the removal of half water molecule (calc. loss=4.15%). There are respective small DTA (endothermic) and DTG peaks at 65°C. A further mass loss of 18% in the second stage suggests the removal of another installment of two water molecules at

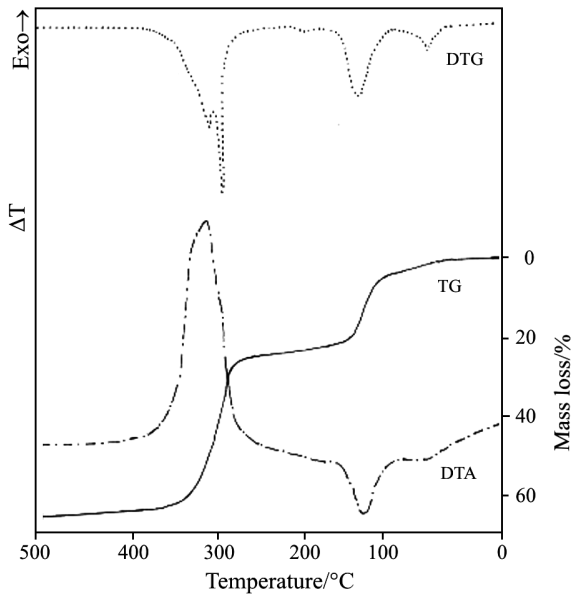

Fig. 8 Simultaneous TG-DTG-DTA curves of ferrous succinate sesterhydrate

150°C (calc. loss=21%). The corresponding DTG peak occurs at 120°C which is endothermic in DTA. The anhydrous compound remains stable upto 265°C and then undergoes an abrupt oxidative decomposition process till a mass loss of 62% is reached at 400°C suggesting the formation of Fe_2O_3 (calc. loss=62.5%). Although DTG shows that this oxidative process occurs in two steps, however TG and DTA exhibit only one step. The presence of iron oxide as α-Fe_2O_3 has been confirmed by XRD powder pattern and Mössbauer spectrum of the final residue.

Cobalt malonate dihydrate, $CoCH_2C_2O_4 \cdot 2H_2O$

Figure 9 shows the simultaneous thermal analysis curves (TG-DTG-DTA) of cobalt malonate dihydrate at a heating rate of 10°C min^{-1}. The compound undergoes decomposition in two steps. The first step is the dehydration which starts at 169 and completes at 234°C as indicated by a mass loss of 18%. DTA and DTG peaks show corresponding peaks at 204 (endothermic) and 202°C, respectively. The anhydrous compound remains stable upto 270°C and then undergoes a rapid decomposition process as shown by a strong exotherm with maximum peak temperature of 325°C, followed by a large DTG peak. Although DTG and DTA (exothermic) curves show a multistep decomposition process, the slope of TG indicates only one major oxidative step leading to the formation of a stable product. The shoulders in DTG and DTA peaks may be due to some short-lived unstable intermediate species which subsequently oxidized to cobalt oxide. Formation of cobalt oxide as the final thermolysis product has been confirmed by XRD

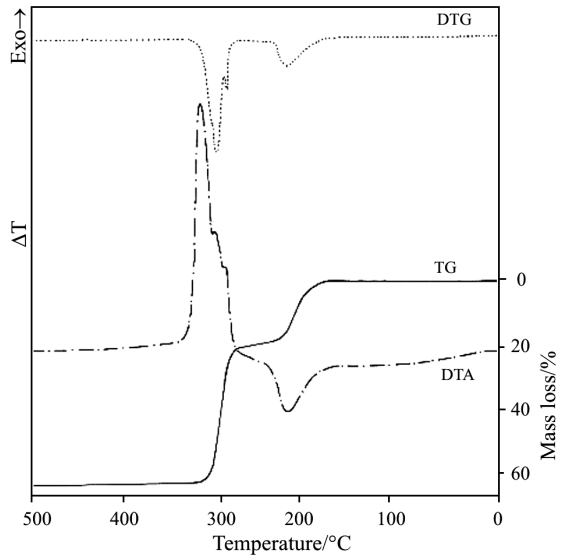

Fig. 9 Simultaneous TG-DTG-DTA curves of cobalt malonate dihydrate

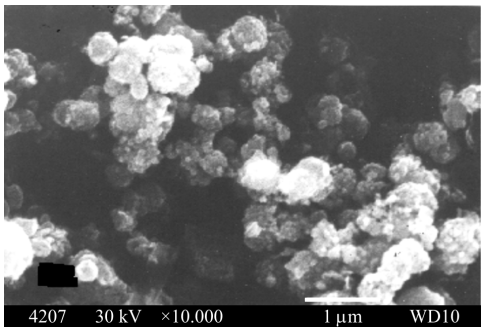

Fig. 10 SEM micrograph of the final thermolysis residue of cobalt malonate dihydrate (CoO), sintered at 400°C for 3 h

powder pattern which agrees to that reported for CoO [15]. IR spectrum of the final residue shows characteristic ν_{Co-O} bands in the range 480–300 cm^{-1}. SEM micrograph (Fig. 10) reveals the formation of CoO with an average particle size of 85 nm.

Cobalt succinate tetrahydrate, $Co(CH_2)_2C_2O_4{\cdot}4H_2O$

Figure 11 shows the simultaneous thermal analysis curves (TG-DTG-DTA) of cobalt succinate tetrahydrate at a heating rate of 10°C min^{-1}. An initial mass loss of only one percent at 51°C may correspond to desorption of the absorbed gases. The compound then undergoes dehydration, which completes at 180°C as shown by a mass loss of 29% (calc. loss=29.2%). The corresponding DTG and DTA (endothermic) peaks both lie at 160°C. The anhydrous compound remains stable upto 330°C and then undergoes an abrupt decomposition process upto 420°C as shown by DTA peak (exothermic) at 372°C. This decomposition process is associated with a mass loss of 69.5% (calc. loss=70%) indicating the formation of cobalt oxide (CoO). Existence of CoO as the final thermolysis products has been confirmed by XRD powder pattern and IR spectrum of the ultimate residue.

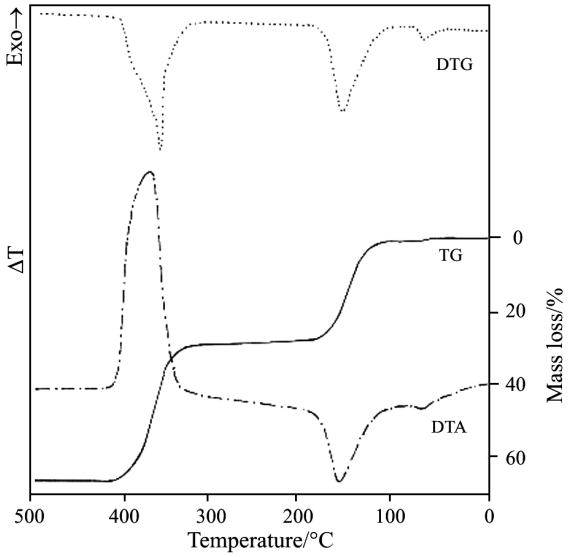

Fig. 11 Simultaneous TG-DTG-DTA curves of cobalt succinate tetrahydrate

Nickel malonate dihydrate, $NiCH_2C_2O_4{\cdot}2H_2O$

The decomposition pattern of nickel malonate dihydrate is almost similar to that observed for its cobalt counterpart.

Nickel succinate tetrahydrate, $Ni(CH_2)_2C_2O_4{\cdot}4H_2O$

Figure 12 shows the simultaneous thermal analysis curves (TG-DTG-DTA) of nickel succinate tetrahydrate at a heating rate of 10°C min^{-1}. The compound undergoes decomposition in two steps. The first step is the dehydration which commences at 114 and completes at 200°C as shown by a mass loss of 29% (calc. loss=29.2%). Corresponding DTA (endothermic) and DTG peaks lie at 153 and 150°C, respectively. The anhydrous compound remains stable upto 380°C and then undergoes an abrupt oxidative decomposition process till a mass loss of 70% is obtained at 450°C indicating the formation of NiO (calc. loss=70.0%). Although DTA shows that this oxidation process occurs in two steps, however TG and DTG (peak temperature 410°C) exihibt only single step. Formation of nickel oxide as the final thermolysis product has been confirmed by XRD powder pattern which agrees to that reported for NiO [16]. IR spectrum shows a characteristic band at 480 cm^{-1} due to ν_{Ni-O} bonding.

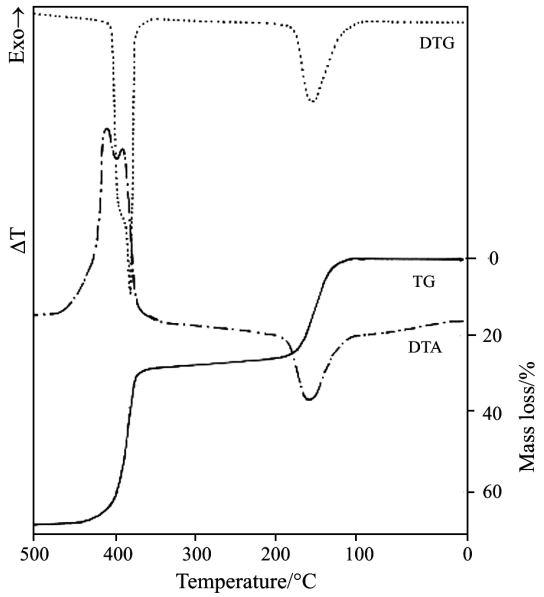

Fig. 12 Simultaneous TG-DTG-DTA curves of nickel succinate tetrahydrate

Copper malonate dihydrate, $CuCH_2C_2O_4 \cdot 2H_2O$

Figure 13 shows the simultaneous thermal analysis curves (TG-DTG-DTA) of copper malonate dihydrate at a heating rate of 10°C min^{-1}. The compound undergoes decomposition in two steps. The first step is dehydration which commences at 107 and is completed at 190°C as indicated by a mass loss of 16%. DTA and DTG show corresponding peaks at 133 (endothermic) and 130°C, respectively. The anhydrous compound remains stable upto 225°C and then undergoes a small endothermic decomposition step which subsequently becomes exothermic indicating that an unstable short-lived intermediate might have oxidized immediately after its formation. DTG also shows a shoulder corresponding to this step. These thermal changes are accompanied by a mass loss of 64.5% at 300°C suggesting the formation of copper(I) oxide, Cu_2O (calc. loss=64.52%). However, Cu_2O formed underwent oxidation above 315°C (as supported by an exotherm) resulting in an increase of mass by approximately 4% due to its transition to copper(II) oxide ($Cu^I \rightarrow Cu^{II}$). The identity of the final thermolysis product has been confirmed by XRD powder pattern which agrees to that reported for CuO [17]. IR spectrum of the final residue also shows a distinct band at 475 cm^{-1} due to ν_{Cu-O} bonding.

Copper succinate dihydrate, $Cu(CH_2)_2C_2O_4 \cdot 2H_2O$

Figure 14 shows the simultaneous thermal analysis curves (TG-DTG-DTA) of copper succinate dihydrate at a heating rate of 10°C min^{-1}. The dehydration starts at 66 and completes at 120°C as shown by a mass loss of 17% in TG (calc. loss=16.7%). There are corresponding broad DTA (endothermic) and DTG peaks centered at 100 and 105°C, respectively. The anhydrous compound remains stable upto 315°C and then undergoes a rapid oxidative pyrolysis till a mass loss of 63% is obtained at 440°C indicating the formation of CuO. The presence of a doublet in DTA and a shoulder in DTG suggests that initially copper(I) oxide (Cu_2O) is formed (as supported by a mass loss of 67% at 355°C), which at higher temperature oxidizes to copper(II) oxide, CuO thereby decreasing the final mass loss to 63% due to oxidation of Cu(I) to Cu(II) state. The existence of CuO as the end product

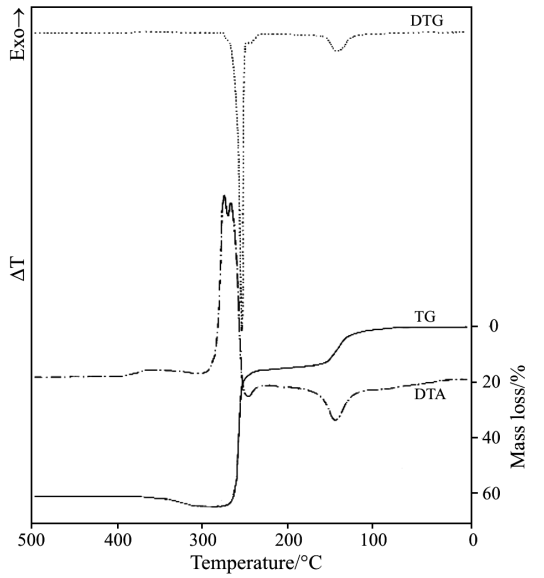

Fig. 13 Simultaneous TG-DTG-DTA curves of copper malonate dihydrate

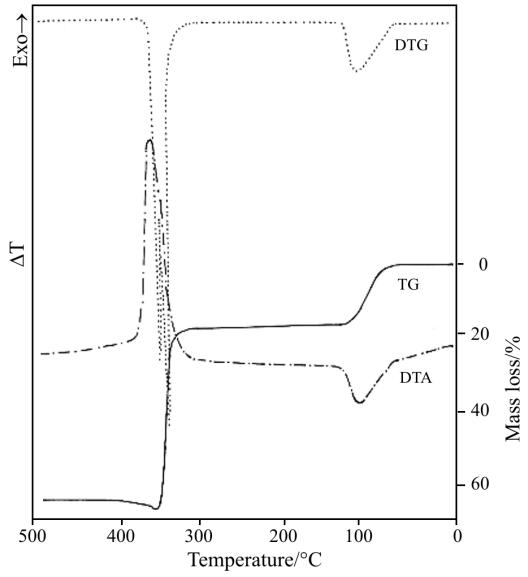

Fig. 14 Simultaneous TG-DTG-DTA curves of copper succinate dihydrate

has been confirmed by XRD powder pattern and IR spectrum of the final residue.

Zinc malonate dihydrates, $ZnCH_2C_2O_4 \cdot 2H_2O$

Figure 15 shows the simultaneous thermal analysis curves (TG-DTG-DTA) of zinc malonate dihydrate at a heating rate of 10°C min^{-1}. The compound undergoes decomposition in two steps. The first step is the dehydration, which commences at 130 and completes at 192°C as indicated by a mass loss of 17% due to the removal of two water molecules (calc. loss=17.7%). DTA and DTG show corresponding peaks at 165 (endothermic) and 170°C, respectively. The anhydrous compound remains stable upto 258°C and then undergoes a rapid decomposition process as shown by a strong exotherm at 305°C followed by a large DTG peak at 310°C. Although DTG shows more than one decomposition stages, TG suggests only a single major step. A mass loss of 60% for this step corresponds to the formation of zinc oxide (calc. loss=60%). The identity of the final thermolysis product has been confirmed by XRD powder pattern which resembles to that reported for ZnO [18]. IR spectrum of the final residue shows a sharp band at 490 cm^{-1} due to ν_{Zn-O} bonding.

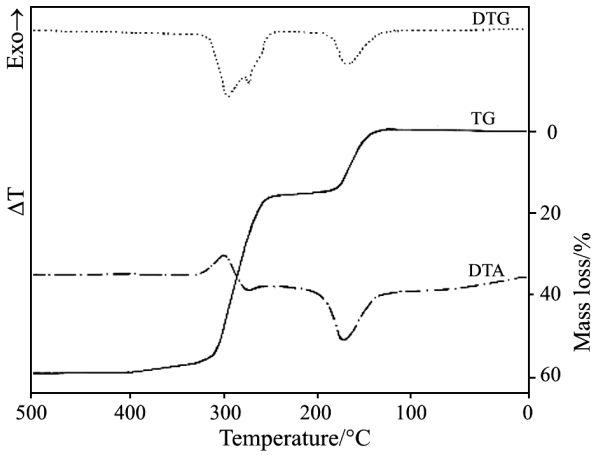

Fig. 15 Simultaneous TG-DTG-DTA curves of zinc malonate dihydrate

Zinc succinate, $Zn(CH_2)_2C_2O_4$

Figure 16 shows the simultaneous thermal analysis curves (TG-DTG-DTA) of zinc succinate at a heating rate of 10°C min^{-1}. Being anhydrous, the compound undergoes decomposition in one step only. After remaining stable upto 428°C, it undergoes an abrupt oxidative decomposition process upto 522°C leading to a mass loss of 55% revealing the formation of ZnO (calc. loss=55.2%). Although DTA and DTG show this oxidative decomposition to be multistep process, TG exhibits only one step. The presence of ZnO as the ultimate product has been confirmed by XRD powder pattern and IR spectrum of the final thermolysis residue.

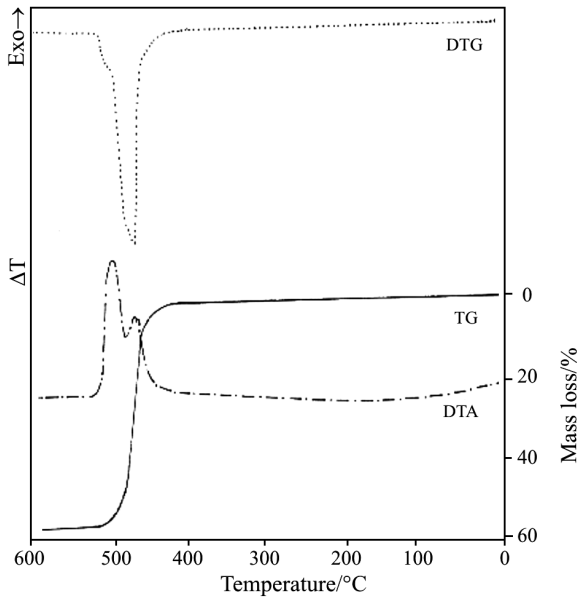

Fig. 16 Simultaneous TG-DTG-DTA curves of zinc succinate

On the basis of various physico-chemical studies, the following mechanisms for the thermolysis of transition metal malonates (A) and succinates (B) in air are proposed:

$$MCH_2C_2O_4 \cdot xH_2O \xrightarrow{\text{dehydration, 190–290°C}} \xrightarrow{\text{dehydration, 190–290°C}} MCH_2C_2O_4 \quad A(i)$$

(M=Mn, Fe, Co, Ni, Cu, Zn)

$$MCH_2C_2O_4 \xrightarrow{\text{decomposition, 325–485°C}} MO(s) + 1/2C_2H_4(g) + 3/2CO(g) + 1/2CO_2(g) \quad A(ii)$$

(M=Mn, Co, Ni, Cu, Zn)

$$FeCH_2C_2O_4 \xrightarrow{\text{decomposition, 484°C}} 1/2\alpha\text{-}Fe_2O_3(s) + 1/2C_2H_4(g) + 3/2CO(g) + 1/2CO_2(g)$$

$$M(CH_2)_2C_2O_4 \cdot xH_2O \xrightarrow{\text{dehydration, 120–215°C}} \xrightarrow{\text{dehydration, 120–215°C}} M(CH_2)_2C_2O_4 \quad B(i)$$

$$M(CH_2)_2C_2O_4 \xrightarrow{\text{decomposition, 400–525°C}} MO(s) + C_2H_4(g) + CO(g) + CO_2(g) \quad B(ii)$$

(M=Mn, Co, Ni, Cu, Zn)

$$Fe(CH_2)_2C_2O_4 \xrightarrow{\text{decomposition, 400°C}} 1/2\alpha\text{-}Fe_2O_3(s) + C_2H_4(g) + 3/2CO(g) + 1/2CO_2(g)$$

Conclusions

Transition metal (M=Mn, Fe, Co, Ni, Cu, Zn) malonates and succinates decompose directly to respective oxides. Transition metal ferricarboxylates [19, 20] have also been reported to decompose directly to their respective oxides. The oxides obtained are nanosized as revealed by SEM analysis.

A comparative study of transition metal succinates and respective malonates reveals the following stability order:

succinates>malonates

The transition metal succinates are thermally more stable than the respective malonates. This is attributed to the fact that two methylene groups present in the succinates prevent the direct interaction between carboxylate groups, thus causing their slow breakdown [21].

References

1 E. Markowicz, Farben-Ztg., (1928) 34,336,414,503.
2 K. N. Mehrotra and S. C. Bhargav, Z. Phys. Chem., 237 (1968) 327; Chem. Abst., 69 (1968) 37364.
3 A.-S. Malik, M. J. Duncan and P. G. Bruce, J. Mater. Chem., 13 (2003) 2123.
4 V. E. Henrich and P. A. Cox, The Surface Science of Metal Oxides, Cambridge University Press, 1994.
5 R. C. Mehrotra and R. Bohra, Metal Carboxylates, Academic Press, New York 1983.
6 D. Dollimore and D. L. Griffiths, J. Thermal Anal., 2 (1970) 229.
7 A. I. Vogel, Quantitative Inorganic Analysis, 3rd Ed., Longman Group Ltd., England 1973.
8 K. Nakamoto, Infrared Spectra of Inorganic and Coordination Compounds, 2nd Ed., John Wiley Intersci., New York 1970.
9 ASTM Card Number 7-230.
10 R. A. Nyguist and R. O. Kagel, Infrared Spectra of Inorganic Compounds, Academic Press, 1971.
11 D. A. Edwards and R. N. Hayward, Can. J. Chem., 46 (1968) 3443.
12 ASTM Card Number 13-534.
13 S. S. Bellad, C. D. Lokhande and C. H. Bhosale, Indian J. Pure Appl. Phys., 35 (1997) 565.
14 B. S. Randhawa and P. S. Bassi, Radiochem. Radioanal. Letts., 59 (1983) 171.
15 ASTM Card Number 9-402.
16 JCPDS Card Number 4-0835.
17 ASTM Card Number 5-0661.
18 ASTM Card Number 5-0664.
19 O. Carp, L. Patron, G. Marinescu, G. Pascu and P. Budrugeac, J. Therm. Anal. Cal., 72 (2003) 263.
20 B. S. Randhawa, K. J. Sweety, Manpreet Kaur and J. M. Greneche, J. Therm. Anal. Cal., 75 (2004) 101.
21 A. K. Galway and M. A. Mohamed, J. Chem. Soc. Faraday, 81 (1985) 2503.

Received: January 20, 2005
Accepted: May 2, 2005
OnlineFirst: December 12, 2005

DOI: 10.1007/s10973-005-7120-y